1   **Discovery of a 382-nt deletion during the early evolution of SARS-CoV-2**

2

3   **Running title:** A SARS-CoV-2 deletion variant

4

5   Yvonne CF Su[1†], Danielle E Anderson[1†], Barnaby E Young[2,3,9‡], Feng Zhu[1‡], Martin

6   Linster[1‡], Shirin Kalimuddin[1,4], Jenny GH Low[1,4], Zhuang Yan[1], Jayanthi Jayakumar[1], Louisa

7   Sun[5], Gabriel Z Yan[6], Ian H Mendenhall[1], Yee-Sin Leo[2,3,7,8,9], David Chien Lye[2,3,8,9], Lin-Fa

8   Wang[1,10*], Gavin JD Smith[1,10*]

9

10   [1]Programme in Emerging Infectious Diseases, Duke-NUS Medical School; [2]National Centre

11   for Infectious Diseases; [3]Tan Tock Seng Hospital; [4]Singapore General Hospital; [5]Alexandra

12   Hospital; [6]National University Hospital; [7]Saw Swee Hock School of Public Health, [8]Yong

13   Loo Lin School of Medicine, [9]Lee Kong Chian School of Medicine, [10]SingHealth Duke-NUS

14   Global Health Institute, Singapore

15

16   [†]These authors contributed equally

17   [‡]These authors contributed equally

18   *To whom correspondence may be addressed. LFW linfa.wang@duke-nus.edu.sg and GJDS

19   gavin.smith@duke-nus.edu.sg.

20 **To date, the SARS-CoV-2 genome has been considered genetically more stable than**

21 **SARS-CoV or MERS-CoV. Here we report a 382-nt deletion covering almost the entire**

22 **open reading frame 8 (ORF8) of SARS-CoV-2 obtained from eight hospitalized patients**

23 **in Singapore. The deletion also removes the ORF8 transcription-regulatory sequence**

24 **(TRS), which in turn enhances the downstream transcription of the N gene. We also**

25 **found that viruses with the deletion have been circulating for at least four weeks.**

26 **During the SARS-CoV outbreak in 2003, a number of genetic variants were observed in**

27 **the human population [1], and similar variation has since been observed across SARS-**

28 **related CoVs in humans and bats. Overwhelmingly these viruses had mutations or**

29 **deletions in ORF8, that have been associated with reduced replicative fitness of the**

30 **virus [2]. This is also consistent with the observation that towards the end of the**

31 **outbreak sequences obtained from human SARS cases possessed an ORF8 deletion that**

32 **may be associated with host adaptation [1]. We therefore hypothesise that the major**

33 **deletion revealed in this study may lead to an attenuated phenotype of SARS-CoV-2.**

34

35 On 1 December 2019, a novel coronavirus emerged from Hubei province in China and

36 infected people visiting the Huanan seafood market in Wuhan [3]. The virus demonstrated

37 efficient human-to-human transmission within mainland China and subsequently spread

38 across many countries. The virus was soon identified as 2019-nCoV, more recently

39 designated SARS-CoV-2, while the disease is referred to as COVID-19. On 30 January 2020,

40 the World Health Organization declared a Public Health Emergency of International

41 Concern. As of 10 March 2020, the COVID-19 outbreak has led to 113,702 confirmed cases

42 and 4,012 deaths globally [4]. Zoonotic viruses have crossed the species barrier from animals

43 to humans and the success of an interspecies transmission is the ability of a novel virus to

44   adapt, via genetic mutation events, to a new host and cause sustained transmission that can

45   lead to a significant outbreak.

46

47   Nasopharyngeal swabs collected from hospitalized patients positive for SARS-CoV-2 in

48   Singapore were subjected to next generation sequencing (NGS) analysis, with and without

49   passaging in Vero-E6 cells. The NGS data revealed a 382-nt deletion towards the 3' end of

50   the viral genomes obtained from multiple patients (Suppl. Table 1). To confirm this

51   observation, specific PCR primers were designed flanking the deleted region and Sanger

52   sequencing performed (Suppl. Fig. 1). This verified the deletion at positions 27,848 to 28,229

53   of the SARS-CoV-2 genome. Interrogation of the NGS assemblies of these 382-nt deletion

54   variants (referred to hereafter as Δ382) indicated that the virus populations were

55   homogenous.

56

57   Apart from the 382-nt deletion, the genome organization of the Δ382 viruses is identical to

58   that of other SARS-CoV-2 (Fig. 1A). Closer examination of the deletion indicated that it

59   spans an area of the ORF7b and ORF8 that includes the ORF8 transcriptional regulator

60   sequence (TRS), eliminating ORF8 transcription (Fig. 1B). The ORF8 region has been

61   identified as an evolutionary hotspot of SARSr-CoVs. For instance, sequences of human

62   SARS-CoV TOR2 and LC2 exhibit 29-nt and 415-nt deletions, whereas those of bat SARS-

63   CoV JTMC15 have discontinuous deletions in ORF7/8 (Fig. 1B) [5-8]. The ORF8 region of

64   SARS-CoVs has been shown to play a significant role in adaptation to the human host

65   following interspecies transmission [7] and virus replicative efficiency [2]. Similarly the

66   disruption of ORF8 region in Δ382 viruses may be a result of human adaptation after the

67   emergence of SARS-CoV-2.

68

69   To investigate the possible effects of the TRS deletion, we calculated and compared the total

70   number of transcripts per million (TPM) of each gene between wild-type (WT) and Δ382

71   viruses. For each gene, we counted unambiguous reads that uniquely mapped to the gene-

72   specific transcripts that include the joint leader and TRS sequences [9]. We analysed three

73   WT and two Δ382 sequences for which two independent NGS library preparations were

74   available. Our results indicate differential patterns of TPM level between WT and Δ382

75   viruses (Fig. 2A). The Δ382 sequences displayed a greater level of TPMs in the ORF6,

76   ORF7a and N genes compared to WT. More specifically, the Δ382 N gene, downstream of

77   ORF8, showed a significant increase in the TPM level. To further determine the impact of the

78   382-nt deletion on the transcription of the N gene, we conducted qPCR to measure the

79   relative abundance of the RNAs from 2 genes (E and N) located upstream and downstream of

80   the deleted region, respectively. Results shown in Figure 2B confirm the enhancement of N

81   gene transcription in Δ382 viruses. This enhancement was consistently observed regardless of

82   the sample type, whether directly from swab samples or passaged viruses.

83

84   The global phylogeny of SARS-CoV-2 (Suppl. Fig. 2) revealed a comb-like appearance in

85   the phylogenetic tree and a general lack of phylogenetic resolution, reflecting the high

86   similarity of the virus genomes. This tree topology is a typical characteristic of a novel

87   interspecies transmission, wherein the viruses are infecting immunologically naïve

88   populations with sustained human-to-human transmission, as previously shown for the early

89   stages of the 2009 H1N1 pandemic [10]. Notably, we observe an emerging virus lineage

90   (tentatively designated as "Lineage 1" in Suppl. Fig. 2) that consists of sequences from

91   various newly affected countries with recent virus introductions. All viruses from this recent

92   lineage possess an amino acid substitution at residue 250 (from lysine to serine) on the ORF8

4

93 gene [11], which is known to undergo strong positive selection during animal-to-human

94 transmission [7].

95

96 To estimate the divergence times among lineages of SARS-CoV-2, we reconstructed a dated

97 phylogeny based on 137 complete genomes, including data from this study. The estimated

98 rate of nucleotide substitutions among SARS-CoV-2 viruses is approximately at 8.68×10^{-4}

99 substitutions per site per year (95% HPD: $5.44 \times 10^{-4} - 1.22 \times 10^{-3}$), which is moderately lower

100 than SARS-CoV ([12]: $0.80 - 2.38 \times 10^{-3}$) and MERS-CoV (with a mean rate [13] of: 1.12×10^{-3}

101 and 95% HPD: $58.76 \times 10^{-4} - 1.37 \times 10^{-3}$) as well as human seasonal influenza viruses (ranging

102 $1.0 - 5.5 \times 10^{-3}$ depending on individual gene segments [10, 14-16]. In contrast, the estimated

103 rate of SARS-CoV-2 viruses is greater than estimates for human coronaviruses by a

104 magnitude order of 4×10^{-4} [17].

105

106 The mean TMRCA estimates indicate the introduction of SARS-CoV-2 into humans (Fig. 3.

107 node A) occurred in the middle of November 2019 (95% HPD: 2019.77–2019.94) (Table 1),

108 suggesting that the viruses were present in human hosts approximately one month before the

109 outbreak was detected. A single amino-acid mutation was fixed on the ORF8 region of all

110 full-genome Lineage 1 viruses (Fig. 3, node B), with the TMRCA estimate of 22 December

111 2019 (95% HPD: 2019.9–2020.0). The Δ382 viruses form a monophyletic group within

112 Lineage 1, and dating estimates indicate that they may have arisen in the human population in

113 Singapore around 07 February 2020 (95% HPD: 2020.12–2020.06), consistent with the date

114 of collection of the Δ382 positive samples (17–19 February 2020). The three Δ382 viruses

115 shared a high level of nucleotide similarities (99.9%) with only 5 nucleotide differences

116 between them. Although the dated phylogeny indicates that Δ382 viruses clustered together

117 and are possibly derived from a single source, there is a general lack of statistical support in

118   SARS-CoV-2 phylogenies due to its recent emergence, and evolutionary inferences should be

119   made with caution.

120

121   In this report we describe the first major evolutionary event of the SARS-CoV-2 virus

122   following its emergence into the human population. Although the biological consequences of

123   this deletion remain unknown, the alteration of the N gene transcription would suggest this

124   may have an impact on virus phenotype. Recent work has indicated that ORF8 of SARS-CoV

125   plays a functional role in virus replicative fitness and may be associated with attenuation

126   during the early stages of human-to-human transmission [2]. Given the prevalence of a

127   variety of deletions in the ORF8 of SARSr-CoVs, it is likely that we will see further deletion

128   variants emerge with the sustained transmission of SARS-CoV-2 in humans. Future research

129   should focus on the phenotypic consequences of $\Delta382$ viruses in the transmission dynamics

130   of the current epidemics and the immediate application of this genomic marker for molecular

131   epidemiological investigation.

132   **Online content.** Any methods, additional references, Nature Research reporting summaries,

133   source data, extended data, supplementary information, acknowledgements, peer review

134   information; details of author contributions and competing interests; and statements of data

135   availability are available at [Article DOI].

136

137   **Data availability.** The new sequences generated in this study have been deposited in

138   GISAID database under accession numbers EPI_ISL_407987, EPI_ISL_407988,

139   EPI_ISL_410535 to EPI_ISL_410537 for WT viruses and EPI_ISL_414378 to

140   EPI_ISL_414380 for Δ382 viruses.

141

153

154   **Author contributions.** YCFS, DEA, LFW, GJDS designed and supervised research. BEY,

155   SK, JGHL, LS, GZY, YSL, DCL collected and provided samples. DEA, ML, YZ conducted

156   experiments. YCFS, ZF, JJ, IHM, GJDS performed analyses. YCFS, ZF, ML, LFW, GJDS

157   wrote the paper. All authors reviewed and approved the manuscript.

158

159   **Methods**

160   **Ethics statement.** This study was undertaken as part of the national disease outbreak and the

161   response and the protocols were approved by the ethics committee of the National Healthcare

162   Group. Patient samples were collected under PROTECT (2012/00917), a multi-centred

163   Prospective Study to Detect Novel Pathogens and Characterize Emerging Infections. Work

164   undertaken at the Duke-NUS Medical School ABSL3 laboratory was approved by the Duke-

165   NUS ABSL3 Biosafety Committee, National University of Singapore and Ministry of Health

166   Singapore.

167

168   **Virus culture, RNA extraction and sequencing.** Clinical samples from infected patients

169   were collected from public hospitals in Singapore from January–February 2020. Material

170   from clinical samples was used to inoculate Vero-E6 cells (ATCC®CRL-1586™). Total RNA

171   was extracted using E.Z.N.A. Total RNA Kit I (Omega Bio-tek) according to manufacturer's

172   instructions and samples analysed by real-time quantitative reverse transcription-PCR (RT-

173   qPCR) for the detection of SARS-CoV-2 as previously described [18]. Whole genome

174   sequencing was performed using next-generation sequencing (NGS) methodology. The

175   cDNA libraries were constructed using TruSeq RNA Library Prep Kit (Illumina) according to

176   the manufacturer's instructions and sequenced on an Illumina MiSeq System. Raw NGS

177   reads were trimmed by Trimmomatic v0.39 [19] to remove adaptors and low-quality bases.

178   Genome sequences were assembled and consensus sequences obtained using the BWA

179   algorithm in UGENE v.33. To verify the presence of the deletion in the SARS-CoV-2

180   genome, we designed two specific PCR primers (F primer: 5'-

181   TGTTAGAGGTACAACAGTACTTT-3' and R primer: 5'-

182   GGTAGTAGAAATACCATCTTGGA-3') targeting the ORF7–8 regions. For samples with

183   low Ct values, a hemi-nested PCR was then performed with primers (5'-

184   TGTTTATAACACTTTGCTTCACA-3') and (5'-GGTAGTAGAAATACCATCTTGGA-

185   3'). The PCR mixture contained the cDNA, primers (10μM each), 10x Pfu reaction buffer

186   (Promega), Pfu DNA polymerase (Promega) and dNTP mix (10mM, Thermo Scientific). The

187   PCR reaction was carried out with the following conditions: 95°C for 2 min, 35 cycles at

188   95°C for 1 min, 52°C for 30 sec, 72°C for 1 min and a final extension at 72°C for 10 min in a

189   thermal cycler (Applied Biosystems Veriti). Deletions in the PCR products were visualized

190   by gel electrophoresis and confirmed by Sanger sequencing. Three full Δ382 genomes were

191   generated and designated BetaCoV/Singapore/12/2020, BetaCoV/Singapore/13/2020 and

192   BetaCoV/Singapore/14/2020 along with five WT SARS-CoV-2 genomes previously

193   generated in our laboratories and deposited in GISAID (see Suppl. Table 1).

194

195   **Genomic characterization.** To characterize and map the deletion regions of SARS-CoV-2

196   viruses, we compared with available SARS-CoV-2 and SARs-CoV related genomes from bat

197   SARs-CoV-JTMC15 (accession number: KY182964) and humans SARs-CoV-Tor 2

198   (accession number: AY274119) and LC2 (accession number: AY394999). The viral genome

199   organizations of Wuhan-Hu-1 (accession number: MN908947) and Singapore SARS-CoV-2

200   (Singapore/2 /2020: EPI_ISL_407987) comprise the following gene order and lengths:

201   ORF1ab (open-reading frame) replicase (21291 nt), spike (S: 3822 nt), ORF3 (828 nt),

202   envelope (E: 228 nt), membrane (M: 669 nt), ORF6 (186 nt), ORF7ab (498 nt), ORF8 (366

203   nt) and nucleocapsid (N: 1260 nt).

204

9

205 To understand possible effects of the TRS deletion on the ORF8 region, we analysed the total

206 number of transcripts per million (TPM) of each gene between wildtype and Δ382 variants.

207 For each gene, unambiguous reads which uniquely mapped to the specific joint leader and

208 TRS sequences are counted. We analysed three patients of SARS-CoV-2 wild type and two

209 patients of SARS-CoV-2 variants and independent NGS library preparations were performed

210 twice for each sample. The Wuhan-Hu-1 was used as the reference sequence for genomic

211 coordinates. Leader RNA sequence is situated at the 5' UTR region of the genome and the

212 core sequence consists of 26 nt: UCU**CUAAACGAA**CUUUAAAAUCUGUG. Each of the

213 coding genes is preceded by a core transcription regulatory sequence (TRS) which is highly

214 conserved (i.e. ACGAAC), resembling the leader core sequence. The leader RNA is joined to

215 the TRS regions of different genes and the joining is required for driving subgenomic

216 transcription. Coding sequence (CDS), leader and TRS sequences annotations were generated

217 in Geneious and followed published SARS-CoV studies [9]. To characterize the differential

218 levels of TRS for each gene, 70 nt leader sequence and 230 nt downstream of each TRS

219 sequence were annotated individually to form a 300bp leader-TRS transcript for the splicing-

220 aware aligners in R package rtracklayer (v 1.44). NGS raw fastq reads were then mapped to

221 the reference genome by Geneious RNA-Seq mapper with the annotation of splice-junctions

222 for the leader-TRS. For each gene, the TPM of leader-TRS was then calculated in Geneious

223 by excluding ambiguous reads which may come from other TRS. The resulting TPM data

224 was generated in Geneious and graphs plotted using ggplot 2 (v3.2.0) in R v3.6.1. Wilcoxon

225 one-sided tests were performed in R to test the significant differences between WT and Δ382

226 samples. We also compared individual Ct values of E and N genes between WT and Δ382

227 viruses using qRT-PCR assays as previously described [18]. Samples used in this analysis

228 included nasopharyngeal swabs from three WT patient samples and both nasopharyngeal

229   swabs and passaged samples from two Δ382 patients (n=7). Significance between groups was

230   assessed using a one-way analysis of variance (ANOVA) in PRISM v8.3.1.

231

232   **Phylogenetic analyses.** All available genomes of SARS-CoV-2 with associated virus

233   sampling dates were downloaded from the GISAID database. Genome sequence alignment

234   was performed and preliminary maximum likelihood phylogenies of complete genome were

235   reconstructed using RAxML with 1,000 bootstrap replicates in Geneious R9.0.3 software

236   (Biomatters Ltd). Any sequence outliers were removed from subsequent analyses. To

237   reconstruct a time-scaled phylogeny, an uncorrelated lognormal relaxed-clock model with an

238   exponential growth coalescent prior and the HKY85+Γ substitution model was used in the

239   program BEAST v1.10.4 [20] to simultaneously estimate phylogeny, divergence times and

240   rates of nucleotide substitution. Four independent Markov Chain Monte Carlo (MCMC) runs

241   of 100 million generations were performed and sampled every 10,000 generations. The runs

242   were checked for convergence in Tracer v1.7 [21] and that effective sampling size (ESS)

243   values of all parameters was >200. The resulting log and tree files were combined after

244   removing appropriate burn-in values using LogCombiner [20], and the maximum clade

245   credibility (MCC) tree was subsequently generated using TreeAnnontator [20].

References:

1. Chinese, S.M.E.C., *Molecular evolution of the SARS coronavirus during the course of the SARS epidemic in China.* Science, 2004. **303**(5664): p. 1666-9.

2. Muth, D., et al., *Attenuation of replication by a 29 nucleotide deletion in SARS-coronavirus acquired during the early stages of human-to-human transmission.* Sci Rep, 2018. **8**(1): p. 15177.

3. Lu, R., et al., *Genomic characterisation and epidemiology of 2019 novel coronavirus: implications for virus origins and receptor binding.* The Lancet, 2020. **395**(10224): p. 565-574.

4. World_Health_Organization. *Coronavirus disease (COVID-2019) situation reports.* 2020 [cited 2020 Mar 2]; Available from: https://www.who.int/emergencies/diseases/novel-coronavirus-2019/situation-reports.

5. Chinese, S.M.E.C., *Molecular evolution of the SARS coronavirus during the course of the SARS epidemic in China.* Science (New York, N.Y.), 2004. **303**(5664): p. 1666-1669.

6. Wang, L.-F., et al., *Review of bats and SARS.* Emerging infectious diseases, 2006. **12**(12): p. 1834-1840.

7. Lau, S.K., et al., *Severe Acute Respiratory Syndrome (SARS) Coronavirus ORF8 Protein Is Acquired from SARS-Related Coronavirus from Greater Horseshoe Bats through Recombination.* J Virol, 2015. **89**(20): p. 10532-47.

8. Xu, L., et al., *Detection and characterization of diverse alpha- and betacoronaviruses from bats in China.* Virol Sin, 2016. **31**(1): p. 69-77.

9. Hussain, S., et al., *Identification of novel subgenomic RNAs and noncanonical transcription initiation signals of severe acute respiratory syndrome coronavirus.* J Virol, 2005. **79**(9): p. 5288-95.

271 10. Su, Y.C.F., et al., *Phylodynamics of H1N1/2009 influenza reveals the transition from*

272   *host adaptation to immune-driven selection.* Nature Communications, 2015. **6**: p.

273   7952.

274 11. Tang, X., et al., *On the origin and continuing evolution of SARS-CoV-2.* National

275   Science Review, 2020.

276 12. Zhao, Z., et al., *Moderate mutation rate in the SARS coronavirus genome and its*

277   *implications.* BMC Evolutionary Biology, 2004. **4**(1): p. 21.

278 13. Cotten, M., et al., *Spread, circulation, and evolution of the Middle East respiratory*

279   *syndrome coronavirus.* mBio, 2014. **5**(1): p. e01062-13.

280 14. Vijaykrishna, D., et al., *The contrasting phylodynamics of human influenza B viruses.*

281   eLife, 2015. **4**: p. e05055.

282 15. Virk, R.K., et al., *Divergent evolutionary trajectories of influenza B viruses underlie*

283   *their contemporaneous epidemic activity.* Proceedings of the National Academy of

284   Sciences, 2020. **117**(1): p. 619-628.

285 16. Rambaut, A., et al., *The genomic and epidemiological dynamics of human influenza A*

286   *virus.* Nature, 2008. **453**(7195): p. 615-619.

287 17. Vijgen, L., et al., *Complete Genomic Sequence of Human Coronavirus OC43:*

288   *Molecular Clock Analysis Suggests a Relatively Recent Zoonotic Coronavirus*

289   *Transmission Event.* Journal of Virology, 2005. **79**(3): p. 1595-1604.

290 18. Corman, V.M., et al., *Detection of 2019 novel coronavirus (2019-nCoV) by real-time*

291   *RT-PCR.* Eurosurveillance, 2020. **25**(3): p. 2000045.

292 19. Bolger, A.M., M. Lohse, and B. Usadel, *Trimmomatic: a flexible trimmer for Illumina*

293   *sequence data.* Bioinformatics, 2014. **30**(15): p. 2114-2120.

294 20. Suchard, M.A., et al., *Bayesian phylogenetic and phylodynamic data integration*

295   *using BEAST 1.10.* Virus Evol, 2018. **4**(1): p. vey016.

296   21.   Rambaut, A., et al., *Posterior Summarization in Bayesian Phylogenetics Using Tracer*

297   *1.7.* Syst Biol, 2018. **67**(5): p. 901-904.

298

299 **Table 1.** TMRCA estimates of major SARS-CoV-2 nodes.

Node	Mean TMRCA	Lower 95% HPD	Upper 95% HPD
A	2019.87 (15 November 2019)	2019.77 (09 October 2019)	2019.94 (11 December 2019)
B	2019.97 (22 Dec 2019)	2019.90 (26 November 2019)	2020.00 (01 January 2020)
C	2020.09 (07 Feb 2020)	2020.06 (24 January 2020)	2020.12 (14 Feb 2020)

300 Abbreviations: TMRCA, time to most recent common ancestor, HPD: highest posterior
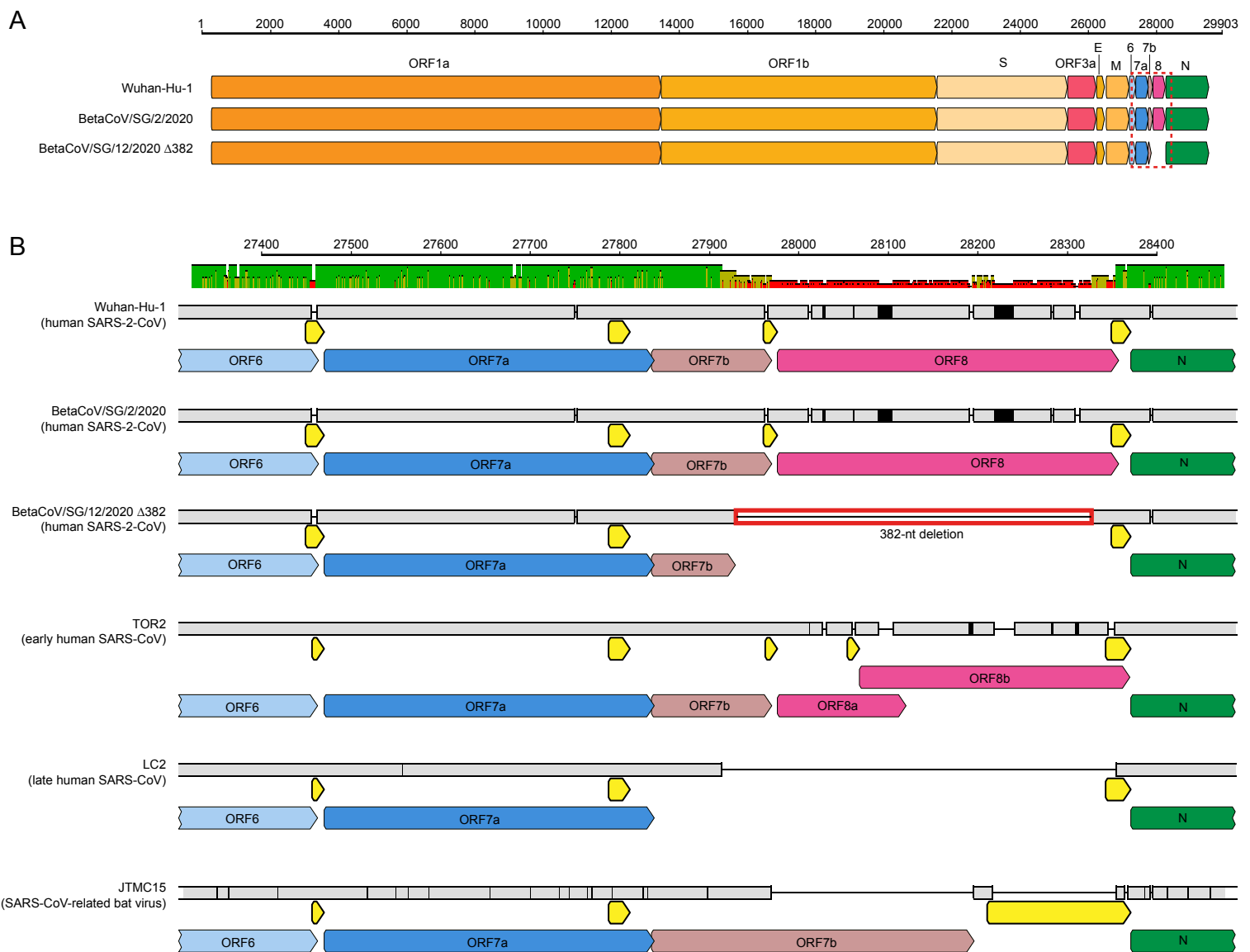
301 density.

Figure 1.

Figure 1. Schematic comparison of SARS-2-CoV, SARS-CoV and SARSr-CoV genomes.
A. Full genome sequences of SARS-2-CoV isolates Wuhan-Hu-1 (GenBank: MN908947), BetaCoV/Singapore/2/2020 (GISAID: 407987), and BetaCoV/Singapore/12/2020 Δ382 (GISAID: EPI_ISL_414378). **B.** Magnification of genomic region (dashed box in Figure 1A), numbers on horizontal axes indicate the nucleotide position relative to Wuhan-Hu-1, grey boxes indicate sequence coverage at a certain position, black horizontal lines represent a deletion at a certain position, open reading frames (ORFs) are indicated by colored arrows. A red-lined box indicates the 382-nt deletion. Transcription-regulatory sequences (TRSs) are indicated by yellow arrows.
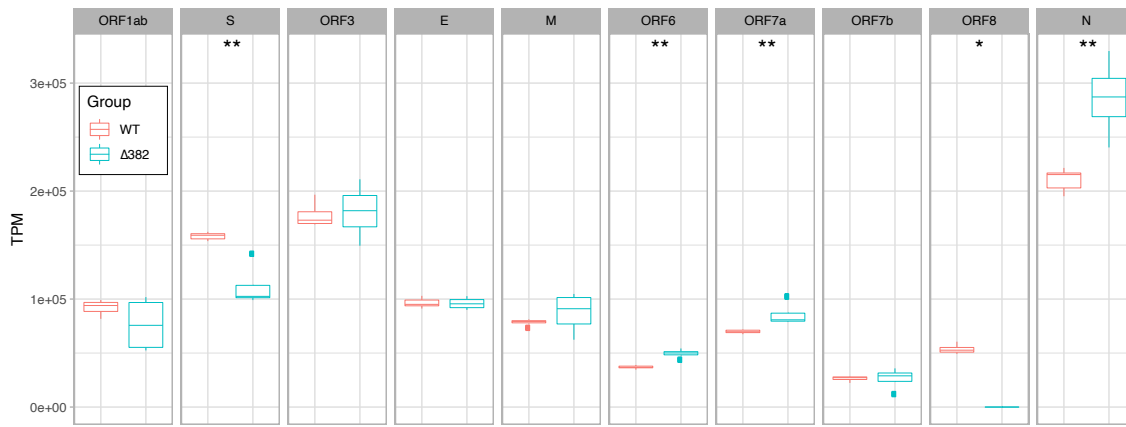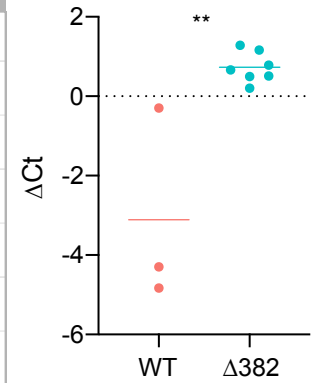
Figure 2. Comparison of transcription of the transcription of the N gene in wild-type (WT) versus Δ382 viruses. A. Abundance of mapped reads relative to transcriptional regulatory sequence (TRS) positions across the genome. 70 bp of leader sequence and 230 of each TRS-downstream sequence were merged in a splice-junction in the annotation. Transcripts per million reads (TPM) was calculated from reads mapped specifically to each leader-TRS region and a whisker and scatter plot was drawn for each gene. A Wilcoxon test was applied to the TPM for each gene of Δ382 to WT (*: p ≤ 0.05 **: p ≤ 0.01). **B.** Relative abundance of the RNAs of the E gene in comparison to the N gene of WT versus Δ382 SARS-CoV-2 (p = 0.002) using qPCR. Horizontal bars indicate the mean of each group.

Figure 3.
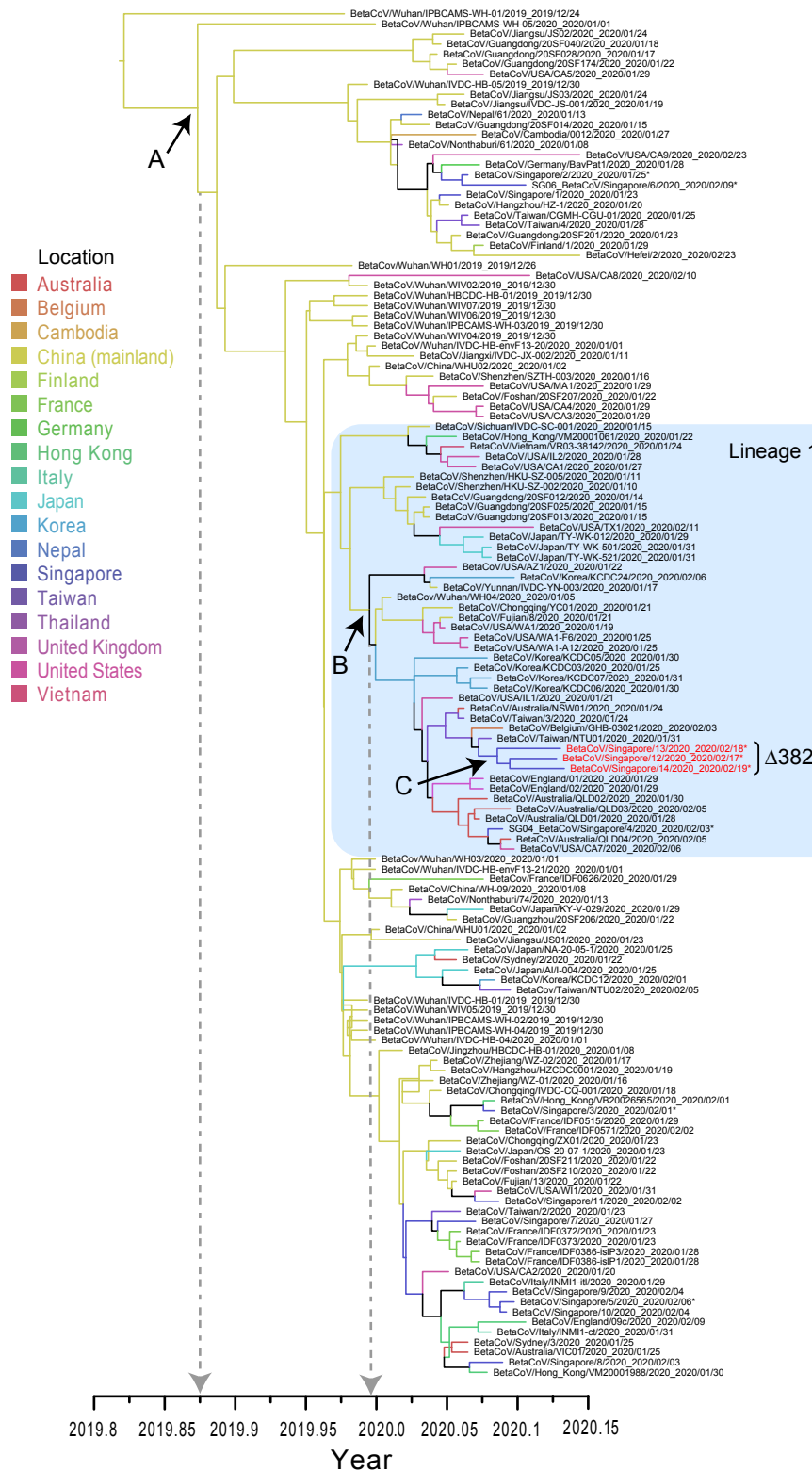
Figure 3. Temporal phylogeny of the complete genomes of SARS-CoV-2 viruses reconstructed using an uncorrelated lognormal relaxed clock model in BEAST. Isolate names in red indicate ∆382 viruses with a large deletion in the ORF7/8 region as described in this study. *Indicates virus genomes generated in this study. Colored branches denote different geographical locations.
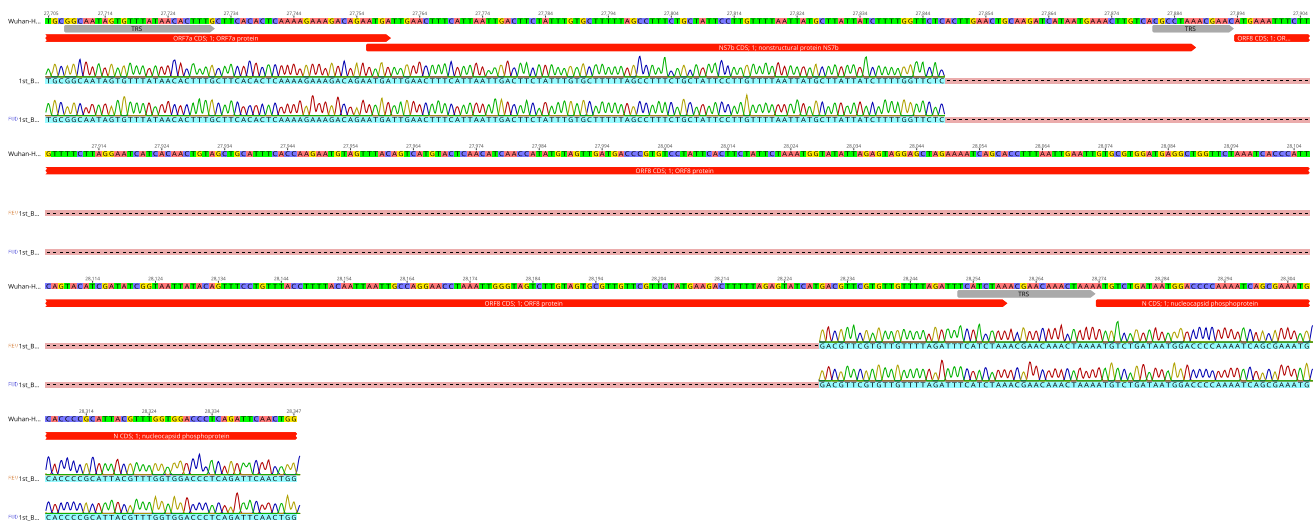
Supplementary Figure 1. Sanger sequences of BetaCoV/Singapore/12/2020 Δ382 mapped to Wuhan-Hu-1 showing the position of the 382-nt deletion in the SARS-CoV-2 genome.
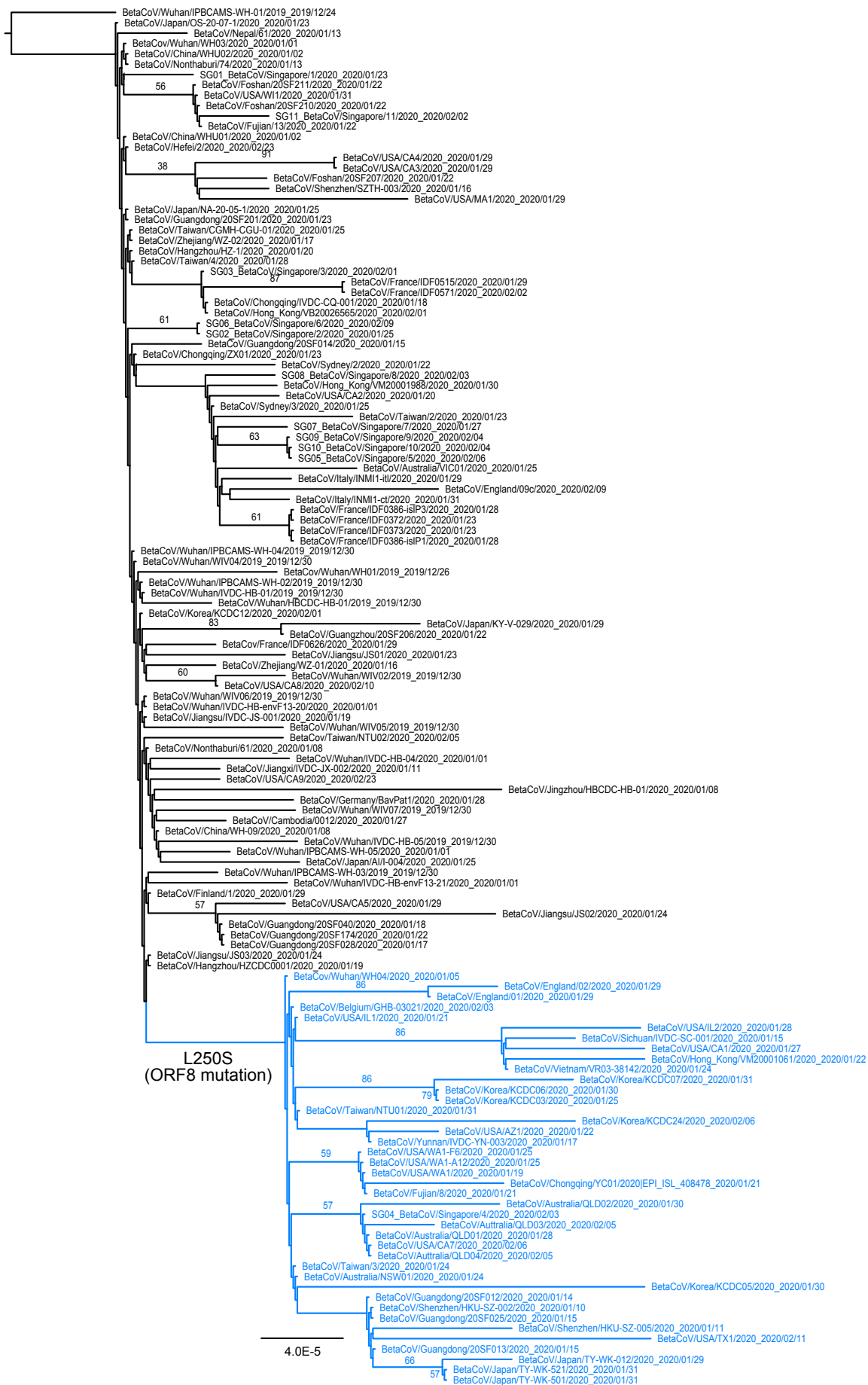
Supplementary Figure 2. Maximum-likelihood tree of SARS-CoV-2 genomes reconstructed using RAxML with 1,000 bootstrap replicates. Δ382 viruses were exlcuded from this analysis as the L250S mutation is located in the ORF8 deletion.

Supplementary Table 1.

Accession number	Virus isolate	Collection date	Note
EPI_ISL_414378	BetaCoV/Singapore/12/2020	17/02/2020	382-nt deletion (this study)
EPI_ISL_414379	BetaCoV/Singapore/13/2020	18/02/2020	382-nt deletion (this study)
EPI_ISL_414380	BetaCoV/Singapore/14/2020	19/02/2020	382-nt deletion (this study)
EPI_ISL_407987	BetaCoV/Singapore/2/2020	25/01/2020	Wild type (this study)
EPI_ISL_407988	BetaCoV/Singapore/3/2020	01/02/2020	Wild type (this study)
EPI_ISL_410535	BetaCoV/Singapore/4/2020	03/02/2020	Wild type (this study)
EPI_ISL_410536	BetaCoV/Singapore/5/2020	06/02/2020	Wild type (this study)
EPI_ISL_410537	BetaCoV/Singapore/6/2020	09/02/2020	Wild type (this study)
EPI_ISL_402119	BetaCoV/Wuhan/IVDC-HB-01/2019	30/12/2019	Wild type
EPI_ISL_402120	BetaCoV/Wuhan/IVDC-HB-04/2020	01/01/2020	Wild type
EPI_ISL_402121	BetaCoV/Wuhan/IVDC-HB-05/2019	30/12/2019	Wild type
EPI_ISL_402123	BetaCoV/Wuhan/IPBCAMS-WH-01/2019	24/12/2019	Wild type
EPI_ISL_402124	BetaCoV/Wuhan/WIV04/2019	30/12/2019	Wild type
EPI_ISL_402127	BetaCoV/Wuhan/WIV02/2019	30/12/2019	Wild type
EPI_ISL_402128	BetaCoV/Wuhan/WIV05/2019	30/12/2019	Wild type
EPI_ISL_402129	BetaCoV/Wuhan/WIV06/2019	30/12/2019	Wild type
EPI_ISL_402130	BetaCoV/Wuhan/WIV07/2019	30/12/2019	Wild type
EPI_ISL_402132	BetaCoV/Wuhan/HBCDC-HB-01/2019	30/12/2019	Wild type
EPI_ISL_403928	BetaCoV/Wuhan/IPBCAMS-WH-05/2020	01/01/2020	Wild type
EPI_ISL_403929	BetaCoV/Wuhan/IPBCAMS-WH-04/2019	30/12/2019	Wild type
EPI_ISL_403930	BetaCoV/Wuhan/IPBCAMS-WH-03/2019	30/12/2019	Wild type
EPI_ISL_403931	BetaCoV/Wuhan/IPBCAMS-WH-02/2019	30/12/2019	Wild type
EPI_ISL_403932	BetaCoV/Guangdong/20SF012/2020	14/01/2020	Wild type
EPI_ISL_403933	BetaCoV/Guangdong/20SF013/2020	15/01/2020	Wild type
EPI_ISL_403934	BetaCoV/Guangdong/20SF014/2020	15/01/2020	Wild type
EPI_ISL_403935	BetaCoV/Guangdong/20SF025/2020	15/01/2020	Wild type
EPI_ISL_403936	BetaCoV/Guangdong/20SF028/2020	17/01/2020	Wild type
EPI_ISL_403937	BetaCoV/Guangdong/20SF040/2020	18/01/2020	Wild type
EPI_ISL_403962	BetaCoV/Nonthaburi/61/2020	08/01/2020	Wild type
EPI_ISL_403963	BetaCoV/Nonthaburi/74/2020	13/01/2020	Wild type
EPI_ISL_404227	BetaCoV/Zhejiang/WZ-01/2020	16/01/2020	Wild type
EPI_ISL_404228	BetaCoV/Zhejiang/WZ-02/2020	17/01/2020	Wild type
EPI_ISL_404253	BetaCoV/USA/IL1/2020	21/01/2020	Wild type
EPI_ISL_404895	BetaCoV/USA/WA1/2020	19/01/2020	Wild type
EPI_ISL_405839	BetaCoV/Shenzhen/HKU-SZ-005/2020	11/01/2020	Wild type
EPI_ISL_406030	BetaCoV/Shenzhen/HKU-SZ-002/2020	10/01/2020	Wild type
EPI_ISL_406031	BetaCoV/Taiwan/2/2020	23/01/2020	Wild type
EPI_ISL_406034	BetaCoV/USA/CA1/2020	27/01/2020	Wild type
EPI_ISL_406036	BetaCoV/USA/CA2/2020	20/01/2020	Wild type
EPI_ISL_406223	BetaCoV/USA/AZ1/2020	22/01/2020	Wild type
EPI_ISL_406531	BetaCoV/Guangdong/20SF174/2020	22/01/2020	Wild type
EPI_ISL_406533	BetaCoV/Guangzhou/20SF206/2020	22/01/2020	Wild type
EPI_ISL_406534	BetaCoV/Foshan/20SF207/2020	22/01/2020	Wild type
EPI_ISL_406535	BetaCoV/Foshan/20SF210/2020	22/01/2020	Wild type
EPI_ISL_406536	BetaCoV/Foshan/20SF211/2020	22/01/2020	Wild type
EPI_ISL_406538	BetaCoV/Guangdong/20SF201/2020	23/01/2020	Wild type
EPI_ISL_406594	BetaCoV/Shenzhen/SZTH-003/2020	16/01/2020	Wild type
EPI_ISL_406597	BetaCoV/France/IDF0373/2020	23/01/2020	Wild type
EPI_ISL_406716	BetaCoV/China/WHU01/2020	02/01/2020	Wild type
EPI_ISL_406717	BetaCoV/China/WHU02/2020	02/01/2020	Wild type
EPI_ISL_406798	BetaCov/Wuhan/WH01/2019	26/12/2019	Wild type
EPI_ISL_406800	BetaCov/Wuhan/WH03/2020	01/01/2020	Wild type
EPI_ISL_406801	BetaCov/Wuhan/WH04/2020	05/01/2020	Wild type
EPI_ISL_406844	BetaCoV/Australia/VIC01/2020	25/01/2020	Wild type
EPI_ISL_406862	BetaCoV/Germany/BavPat1/2020	28/01/2020	Wild type
EPI_ISL_406970	BetaCoV/Hangzhou/HZ-1/2020	20/01/2020	Wild type
EPI_ISL_406973	BetaCoV/Singapore/1/2020	23/01/2020	Wild type
EPI_ISL_407071	BetaCoV/England/01/2020	29/01/2020	Wild type

EPI_ISL_407073	BetaCoV/England/02/2020	29/01/2020	Wild type
EPI_ISL_407079	BetaCoV/Finland/1/2020	29/01/2020	Wild type
EPI_ISL_407084	BetaCoV/Japan/AI/I-004/2020	25/01/2020	Wild type
EPI_ISL_407193	BetaCoV/Korea/KCDC03/2020	25/01/2020	Wild type
EPI_ISL_407214	BetaCoV/USA/WA1-A12/2020	25/01/2020	Wild type
EPI_ISL_407215	BetaCoV/USA/WA1-F6/2020	25/01/2020	Wild type
EPI_ISL_407313	BetaCoV/Hangzhou/HZCDC0001/2020	19/01/2020	Wild type
EPI_ISL_407893	BetaCoV/Australia/NSW01/2020	24/01/2020	Wild type
EPI_ISL_407894	BetaCoV/Australia/QLD01/2020	28/01/2020	Wild type
EPI_ISL_407896	BetaCoV/Australia/QLD02/2020	30/01/2020	Wild type
EPI_ISL_407976	BetaCoV/Belgium/GHB-03021/2020	03/02/2020	Wild type
EPI_ISL_408008	BetaCoV/USA/CA3/2020	29/01/2020	Wild type
EPI_ISL_408009	BetaCoV/USA/CA4/2020	29/01/2020	Wild type
EPI_ISL_408010	BetaCoV/USA/CA5/2020	29/01/2020	Wild type
EPI_ISL_408430	BetaCoV/France/IDF0515/2020	29/01/2020	Wild type
EPI_ISL_408431	BetaCov/France/IDF0626/2020	29/01/2020	Wild type
EPI_ISL_408478	BetaCoV/Chongqing/YC01/2020	21/01/2020	Wild type
EPI_ISL_408479	BetaCoV/Chongqing/ZX01/2020	23/01/2020	Wild type
EPI_ISL_408480	BetaCoV/Yunnan/IVDC-YN-003/2020	17/01/2020	Wild type
EPI_ISL_408481	BetaCoV/Chongqing/IVDC-CQ-001/2020	18/01/2020	Wild type
EPI_ISL_408484	BetaCoV/Sichuan/IVDC-SC-001/2020	15/01/2020	Wild type
EPI_ISL_408486	BetaCoV/Jiangxi/IVDC-JX-002/2020	11/01/2020	Wild type
EPI_ISL_408488	BetaCoV/Jiangsu/IVDC-JS-001/2020	19/01/2020	Wild type
EPI_ISL_408489	BetaCoV/Taiwan/NTU01/2020	31/01/2020	Wild type
EPI_ISL_408514	BetaCoV/Wuhan/IVDC-HB-envF13-20/2020	01/01/2020	Wild type
EPI_ISL_408515	BetaCoV/Wuhan/IVDC-HB-envF13-21/2020	01/01/2020	Wild type
EPI_ISL_408665	BetaCoV/Japan/TY-WK-012/2020	29/01/2020	Wild type
EPI_ISL_408666	BetaCoV/Japan/TY-WK-501/2020	31/01/2020	Wild type
EPI_ISL_408667	BetaCoV/Japan/TY-WK-521/2020	31/01/2020	Wild type
EPI_ISL_408668	BetaCoV/Vietnam/VR03-38142/2020	24/01/2020	Wild type
EPI_ISL_408669	BetaCoV/Japan/KY-V-029/2020	29/01/2020	Wild type
EPI_ISL_408670	BetaCoV/USA/WI1/2020	31/01/2020	Wild type
EPI_ISL_408976	BetaCoV/Sydney/2/2020	22/01/2020	Wild type
EPI_ISL_408977	BetaCoV/Sydney/3/2020	25/01/2020	Wild type
EPI_ISL_409067	BetaCoV/USA/MA1/2020	29/01/2020	Wild type
EPI_ISL_410045	BetaCoV/USA/IL2/2020	28/01/2020	Wild type
EPI_ISL_410218	BetaCov/Taiwan/NTU02/2020	05/02/2020	Wild type
EPI_ISL_410301	BetaCoV/Nepal/61/2020	13/01/2020	Wild type
EPI_ISL_410531	BetaCoV/Japan/NA-20-05-1/2020	25/01/2020	Wild type
EPI_ISL_410532	BetaCoV/Japan/OS-20-07-1/2020	23/01/2020	Wild type
EPI_ISL_410545	BetaCoV/Italy/INMI1-itl/2020	29/01/2020	Wild type
EPI_ISL_410546	BetaCoV/Italy/INMI1-ct/2020	31/01/2020	Wild type
EPI_ISL_410713	BetaCoV/Singapore/7/2020	27/01/2020	Wild type
EPI_ISL_410714	BetaCoV/Singapore/8/2020	03/02/2020	Wild type
EPI_ISL_410715	BetaCoV/Singapore/9/2020	04/02/2020	Wild type
EPI_ISL_410716	BetaCoV/Singapore/10/2020	04/02/2020	Wild type
EPI_ISL_410717	BetaCoV/Australia/QLD03/2020	05/02/2020	Wild type
EPI_ISL_410718	BetaCoV/Australia/QLD04/2020	05/02/2020	Wild type
EPI_ISL_410719	BetaCoV/Singapore/11/2020	02/02/2020	Wild type
EPI_ISL_410720	BetaCoV/France/IDF0372/2020	23/01/2020	Wild type
EPI_ISL_411060	BetaCoV/Fujian/8/2020	21/01/2020	Wild type
EPI_ISL_411066	BetaCoV/Fujian/13/2020	22/01/2020	Wild type
EPI_ISL_411218	BetaCoV/France/IDF0571/2020	02/02/2020	Wild type
EPI_ISL_411219	BetaCoV/France/IDF0386-islP1/2020	28/01/2020	Wild type
EPI_ISL_411220	BetaCoV/France/IDF0386-islP3/2020	28/01/2020	Wild type
EPI_ISL_411902	BetaCoV/Cambodia/0012/2020	27/01/2020	Wild type
EPI_ISL_411915	BetaCoV/Taiwan/CGMH-CGU-01/2020	25/01/2020	Wild type
EPI_ISL_411926	BetaCoV/Taiwan/3/2020	24/01/2020	Wild type
EPI_ISL_411927	BetaCoV/Taiwan/4/2020	28/01/2020	Wild type
EPI_ISL_411950	BetaCoV/Jiangsu/JS01/2020	23/01/2020	Wild type
EPI_ISL_411952	BetaCoV/Jiangsu/JS02/2020	24/01/2020	Wild type

EPI_ISL_411953	BetaCoV/Jiangsu/JS03/2020	24/01/2020	Wild type
EPI_ISL_411954	BetaCoV/USA/CA7/2020	06/02/2020	Wild type
EPI_ISL_411955	BetaCoV/USA/CA8/2020	10/02/2020	Wild type
EPI_ISL_411956	BetaCoV/USA/TX1/2020	11/02/2020	Wild type
EPI_ISL_411957	BetaCoV/China/WH-09/2020	08/01/2020	Wild type
EPI_ISL_412026	BetaCoV/Hefei/2/2020	23/02/2020	Wild type
EPI_ISL_412028	BetaCoV/Hong_Kong/VM20001061/2020	22/01/2020	Wild type
EPI_ISL_412029	BetaCoV/Hong_Kong/VM20001988/2020	30/01/2020	Wild type
EPI_ISL_412030	BetaCoV/Hong_Kong/VB20026565/2020	01/02/2020	Wild type
EPI_ISL_412116	BetaCoV/England/09c/2020	09/02/2020	Wild type
EPI_ISL_412459	BetaCoV/Jingzhou/HBCDC-HB-01/2020	08/01/2020	Wild type
EPI_ISL_412862	BetaCoV/USA/CA9/2020	23/02/2020	Wild type
EPI_ISL_412869	BetaCoV/Korea/KCDC05/2020	30/01/2020	Wild type
EPI_ISL_412870	BetaCoV/Korea/KCDC06/2020	30/01/2020	Wild type
EPI_ISL_412871	BetaCoV/Korea/KCDC07/2020	31/01/2020	Wild type
EPI_ISL_412872	BetaCoV/Korea/KCDC12/2020	01/02/2020	Wild type
EPI_ISL_412873	BetaCoV/Korea/KCDC24/2020	06/02/2020	Wild type